ISSN 2310-6697
otoiser—open transactions on independent scientific-engineering research

FUNKTECHNIKPLUS # JOURNAL

Théorie—Expérimentation—Métrologie—Logiciel—Applications

ISSUE 38 — TUESDAY 30 SEPTEMBER 2025 — YEAR 13

This small European Journal is
In the Defense of Honesty in Science and Ethics in Engineering

Period B'
Previous Period 2013-2024

Publisher

otoiser—open transactions on independent scientific engineering research
ARG IAOI NFI Lab—Antennas Research Group Informal Association Of Individuals No Finance Involved Laboratory
Scheiblingkirchen, Austria

Language — We emphasize the European Origins of our Journal by using English, German and French in its title, as well as, a Hellenic vignette in the front page. However, since we recognize the dominance of US English in the technical literature, we adopted it as the Journal's language.

Focus — We consider Radio—FUNK, which still creates a vivid impression of the untouchable, and its Technology—TECHNIK, from an Advanced—PLUS point of view, Plus—PLUS Telecommunications Engineering, Electrical Engineering and Computer Science, that is, we dynamically focus at any related scientific-engineering research regarding Théorie, Expérimentation, Métrologie, Logiciel, ou Applications.

Scope — We emphasize the scope broadness by extending the title of the Journal with a Doppelkreuz-Zeichen # which we use as a placeholder for the substitution of its disciplines

Frequency — Excluding *forces majeures,* we publish 3 issues per year: on 31st of January, on 31st of May, and on 30th of September.

Editions — We increase the edition number of an issue only when is absolutely needed to reform one or more of its papers——thus to increase their version numbers——but we keep unchanged its 1st edition date shown on its front page and we number its pages sequentially from 1. We count the editions of *About* separately.

Format — We use a fixed-space font, hyphenation, justification, unfixed word spacing, and the uncommon for Journals **A5** (half A4) page size to achieve WYSIWYG printing and clear reading of 2 to 4 side-by-side pages on wide-screen displays.

Editorial Group

Submissions

We can only consider papers written in the preferable and recommended odt format of LibreOffice, or even a paper in the MS Office with MathType doc format, if it would be proved that it is fully compatible with LibreOffice indeed.

Legal Notice — It is taken for granted that the submitter—correspondent author accepts, without any reservation, the totality of our publication conditions as they are analytically detailed here, in this *About*, as well as, that he also carries, in the case of a paper by multiple authors, the independent will of each one of his co-authors to unreservedly accept all the aforementioned conditions for their paper.

Electronic Publishing

We regularly use the Free Libre Open Source Software Libre Office with the Free Liberation Mono font and the Freewares PDFCreator and PDF-Xchange Viewer. We also use some basic html code of ours and the Free Open Digital Library of Internet Archive website, where we upload the FTP#J Collection of Issues, Paper reprints, *About* documents, and Volumes, in both portrait and landscape orientations, for download or very clear online reading with the Free Open Source BookReader.

Internet Addresses

Submissions : sub@ftpj.otoiser.org
Send Updates : updates@ftpj.otoiser.org

Paper Template : https://www.template.ftpj.otoiser.org
Reference Updates : https://www.updates.ftpj.otoiser.org

Internet Publishing : https://www.ftpj.otoiser.org

The FTP#J Collection at Internet Archive Digital Library :
https://archive.org/details/@funktechnikplusjournal

Please download the latest *About* edition from
https://about.ftpj.otoiser.org

Partial Discharges (PD), Pedersen's Model of PD in Enclosed Voids and Some Thoughts on PD Detection Sensitivity

M. G. Danikas and R. Sarathi

Democritus University of Thrace, Department of Electrical and Computer Engineering, 67100 Xanthi, Greece [1]

Indian Institute of Technology Madras, Department of Electrical Engineering, High Voltage Laboratory, Chennai, 600-036 India [2]

Abstract

Partial discharges (PD) may cause deterioration in insulation materials and systems and thus they are considered as one of the main reasons for their ageing. In this paper some comments are offered on a partial discharge model proposed by Pedersen and his colleagues. A brief description is also offered on other PD mechanisms.

Keywords

Partial discharges, insulating materials, PD detection sensitivity, void discharge, PD magnitude, dielectric sample, enclosed void

Introduction

There is a huge amount of technical literature on PD [1] - [4]. Various models explaining the PD behavior have been proposed regarding the different PD mechanisms [5] - [7]. Some of the PD mechanisms have been discussed and analyzed in [8] - [12]. Needless to say that PD very often are the cause of insulation deterioration [13] - [15]. Furthermore, a variety of techniques has been developed in order to detect and register PD activity [16] - [18].

In the context the present paper, brief comments of some PD mechanisms will be given as well some equations relating the applied high-voltage electric field on an insulating sample with the void radius of that sample.

Pedersen's model of PD in enclosed voids

In contradistinction to the traditional approach of the capacitance model of the enclosed void in solid insulation [19], [20], Pedersen and colleagues proposed a more elaborate model based on electromagnetic theory [21]. Pedersen's model expresses the charge q induced on the measuring electrode by the partial discharge in a void in terms of the void geometric factor k, the void volume Ω, the inception electric field for streamer inception E_i, the limiting electric field for ionization E_l, the relative permittivity of the surrounding solid insulating material ε_r, the permittivity of free space ε_0, and dλ/dx the function which gives the ratio of the electric field at the position of the void (in the absence of the void) to the voltage between the electrodes [21] - [23], i.e.

$$q = k\Omega\,\varepsilon_r\,\varepsilon_0\,(E_i - E_l)\,d\lambda/dx \quad (1)$$

(It has to be noted that the term dλ/dx is the same with the term $\nabla\lambda_0$ in the seminal paper [21]). The quantity $(E_i - E_l)$ is expressed in terms of the streamer criterion with the following equation

$$E_i = (1 + B/\sqrt{2\alpha p})\,E_l/p \qquad (2)$$

where, B is a constant characteristic for the gas in the void (B = 8.6 $(\mathrm{m\,Pa})^{1/2}$ for air), α is the radius of the void and p is the pressure in the void. As was noted in [23], the merit of (1) is that the charge q is related to a number of parameters, which affect indeed the void behavior. It is true that Pedersen's model takes into account streamer-type discharges and not Townsend-type discharges (called also subcritical streamer avalanches, with charges below the critical streamer charge of 10^8 e). Pedersen's model does not take into account the thermal discharges (which occur if the charge flowing through the streamer channel is high enough to heat the gas in the channel, so that a significant increase of conductivity may happen either because of thermal detachment of negative ions or because of an increased collisional ionization owing to a decrease of the electric field in the channel by expansion or because of thermal ionization [24]). Pedersen's model leaves out also the swarming micro-discharges, which despite their very small magnitude are not always innocuous [25].

Some scaling relationships

Considering a spherical void inside a solid dielectric, we have that

$$E_v = 3\varepsilon_r E_0/(2\varepsilon_r + 1) + E_{sf} \quad (3)$$

with E_v the electric field inside the void, E_0 the electric field applied to the dielectric sample, ε_r the permittivity of the dielectric and E_{sf} the electric field due to surface charges deposited on the void surface from previous discharges. E_{sf} depends on previous discharges and is usually a quenching field.

Since we consider spherical voids for the simplicity of our calculations, the void volume Ω is expressed as $\Omega = 4\pi\alpha^3/3$, with α the void radius. Consequently, (1) becomes

$$q = [k\, 4\pi\alpha^3 \varepsilon_r \varepsilon_0 (E_i - E_l)\, d\lambda/dx]/3 \quad (4)$$

By introducing in the above relationship the simplified form of (3) (i.e. $E_v = 3\varepsilon_r E_0/(2\varepsilon_r + 1)$), and by bearing in mind that E_v (the field inside the void) is identical with E_i of (1), we finally obtain that

$$E_0 = ([2\varepsilon_r + 1]/3\varepsilon_r)[q/[\varepsilon_r \varepsilon_0 k\, (4/3)\, \pi\alpha^3\, d\lambda/dx]\ \alpha^3] + E_l]] \quad (5)$$

getting thus a direct relationship between the applied electric field to the dielectric sample E_0 with the radius α of the spherical void. Moreover, and this is perhaps even more important, we obtain a relation between the applied field to the dielectric sample at which a void discharge occurs and the void radius for given values of the detecting apparatus sensitivity [24]. In other words, based on (5), we may be able to compare different detecting apparatus sensitivities for given void radii. From (5), we may deduce if a certain applied field E_0 applied to a dielectric sample gives PD detectable signals, i.e. we may also deduce the size of void in the sample. We conclude that the above relation (5), although it is based solely on the streamer criterion, may provide a useful tool for the study and comparison of the PD detecting sensitivities of various PD detecting devices. Needless to say that (5), with the appropriate choice of the characteristic constant for the gas in the void (e.g. SF_6 instead of air), one may also apply the above (5) to spacers for gas-insulated systems (GIS). Pedersen’s model

can also be used - in line with previous publications [26] - in studying the relationship of PD magnitudes to the sensitivity of PD detectors.

The importance of the above should be emphasized: not only PD detector sensitivities can be compared for a given void radius, but also the above imply that thicker insulation needs more sensitive PD detecting equipment. This is of significant industrial importance, especially in environments where external interference is not to be ignored [27] – [29].

Conclusion

In this research note, some comments were offered on Pedersen’s model on partial discharges in enclosed voids. Simple calculations may lead to some useful relations between the radius of an enclosed spherical void with the applied electric field to the dielectric sample containing the void. Such relations may in turn supply with ample information the researcher regarding the comparison of PD sensitivities from various PD detectors for a given enclosed void radius.

References – Updates – MD5 check

https://www.ftpj.otoiser.org/refs/381.htm

[1] Mason J. H., "Discharges", IEEE Transactions on Electrical Insulation, Vol. 13, No. 4, 1978, pp. 211 - 238

[2] Devins J. C., "The physics of partial discharges in solid dielectrics", IEEE Transactions on Electrical Insulation, Vol. 19, No. 5, 1984, pp. 475 - 495

[3] Bartnikas R., "A commentary on partial discharge measurement and detection", IEEE Transactions on Electrical Insulation, Vol. 22, No. 5, 1987, pp. 629 - 653

[4] Burgener H.-P., "Das teilentlandungsverhalten in Mikrohohlauemen polymerer Isoliermaterialien", Ph. D. Thesis, ETH Zuerich, Institut fuer Energieuebertragung und Hochspannungstechnologie, Zuerich, Schweiz, 2003

[5] Kelen A., "Studies on partial discharges on solid dielectrics – A contribution to the discharge resistance testing of insulating materials", Acta Polytechnica Scandinavica, Electrical Engineering series No. 16, Monograph, Total number Pages 138, Stockholm, Sweden, 1967

[6] Kind D., Koenig D., "Untersuchumgen an Epoxidharzpruef-lingen mit kuenstlichen Hohlrauemen bei Wechselspan-nungsbeanspruchung", Elektrie, Vol. 21, 1967, pp. 9 - 13

[7] Morshuis P. H. F., "Partial discharge mechanisms in voids related to dielectric degradation", IEE Proceed-ings on Science, Measurement and Technology (Special Issue on Partial Discharges), Vol. 142, No. 1, 1995, pp. 62 - 68

[8] Bartnikas R., Novak J. P., "On the spark to pseudoglow and glow transition mechanism and discharge detec-tability", IEEE Transactions on Electrical Insulation, Vol. 27, No. 1, 1992, pp. 3 - 14

[9] Danikas M. G., Bartnikas R., Novak J. P., "Discussion on: On the spark to pseudoglow and glow transition mechanism and discharge detectability", IEEE Transac-tions on Electrical Insulation, Vol. 28, No. 3, 1993, pp. 429 - 431

[10] Bartnikas R., Novak J. P., "Different forms of partial discharge and their terminology", IEEE Transactions on Electrical Insulation, Vol. 28, No. 6, 1993, pp. 956 - 968

[11] Danikas M. G., "The definitions used for partial dis-charge phenomena", IEEE Transactions on Electrical In-sulation, Vol. 28, No. 6, 1993, pp. 1075 - 1081

[12] Danikas M. G., "Small partial discharges and their role in insulation deterioration", IEEE Transactions on Die-lectrics and Electrical Insulation, Vol. 4, No. 6, 1997, pp. 863 - 867

[13] Bartnikas R., d' Ombrain G. L., "A study of corona dis-charge rate and ebergy loss in spark gaps", IEEE Tran-sactions on Power Apparatus and Systems, Vol. 84, No. 9, 1965, pp. 770 - 778

[14] Gallagher T. J., Pearmain A. J., "High Voltage – Measu-rement, Testing and Design", Eds. John Wiley & Sons, New York, USA, 1983, Ch. 2, 3 and 4

[15] Kuffel E., Zaengl W. S., Kuffel J., "High Voltage En-gineering: Fundamentals", Eds, Newnes, Oxford, UK, 2000, Ch. 5 and 6

[16] Gulski E., "Computer-aided recognition of partial dis-charges using statistical tools", Ph. D. Thesis, Delft University of Technology, Delft, The Netherlands, 1991

[17] Krivda A., "Recognition of discharges", Ph. D. Thesis, Delft University of Technology, Delft, The Netherlands, 1995

[18] Fromm U., "Partial discharge and breakdown testing at high DC voltage", Ph. D. Thesis, Delft University of Technology, Delft, The Netherlands, 1995

[19] Gemant A., "Die Verlustkurve lufthaeltiger Isolier-stoffe", Zeitschrift fuer Physik, Vol. 13, 1932, pp. 184 - 189

[20] Gemant A., von Philippoff W., "Die Funkestrecke mit Vorkodensator", Zetschrift fuer Physik, Vol. 13, 1932, pp. 425 - 430

[21] Crichton G. C., Karlsson P. W., Pedersen A., "Partial discharges in ellipsoidal and spheroidal voids", IEEE Transactions on Electrical Insulation, Vol. 24, No. 2, 1989, pp. 335 - 342

[22] Boggs S. A., "Partial discharge – Part III: cavity-induced PD in solid dielectrics", IEEE Electrical In-sulation Magazine, Vol. 6, No. 6, 1990, pp. 11 - 20

[23] Danikas M. G., Vardakis G. E., "The case of Pedersen's theory to model partial discharges in cavities enclosed in solid insulations: A criticism of some of its as-pects from an electrical engineers' and from a phy-sicists' point of view", Journal of Electrical En-gineering, Vol. 52, No. 5-6, 2001, pp. 166 - 170

[24] Niemeyer L., Private Correspondence, 1990

[25] Danikas M. G., Adamidis G., "Partial discharges in epo-xy resin voids and the interpretational possibilities and limitations of Pedersen's model", Archiv fuer Elek-trotechnik, Vol. 80, 1997, pp. 105 - 110

[26] Danikas M. G., Vassiliadis G. E., "Models of partial discharges (PD) in enclosed cavities in solid die-lectrics: A study of the relationship of PD magnitudes to the sensitivity of PD detectors and some further comments on insulation lifetime", Journal of Electrical Engineering, Vol. 54, No. 5-6, 2003, pp. 132 - 135

[27] Danikas M. G., "Some possible new applications of a partial discharge (PD) model and its relation to PD detection sensitivity", European Transactions of Elec-trical Power (ETEP), Vol. 6, No. 6, 1996, pp. 445 - 448

[28] Danikas M. G., "Some new relationships and a scaling law regarding partial discharges in spherical cavities enclosed in solid insulation", Acta Electrotehnica Napocensis, Vol. 39, No. 1, 1998, pp. 5 - 9

[29] Danikas M. G., "On some new relationships regarding partial discharges in cylindrical cavities enclosed in solid insulation with their axis perpendicular to the applied electric field", Scientific Bulletin University Politehnica of Bucarest, Series C: Electrical Engineering, Vol. 61, No. 3-4, 1999, pp. 107 - 111

[This Page Intentionally Left Blank]

Various Loads as Calibration Standards for Vector Network Analyzer Measurements

N. I. Yannopoulou and P. E. Zimourtopoulos

Antennas Research Group, Austria - www.op4.eu

Abstract

Preparing Vector Network Analyzer (VNA) measurements we use a handheld multimeter to check if a matching load is defective or damaged. Could we salvage such loads by using them as non-matching VNA calibration standards? In this paper, we present our simple technique we apply to estimate that, by demonstrating the measurement results of various loads, regardless of their operational state, all claiming to be of the same nominal matching value. Our evaluation is both direct and indirect, by respectively considering each of them, either as a Device Under Test (DUT) or as a Standard with DUT the constructed by us DC Resistance Box that we steadily use for reference. Notably, the measurements were conducted in different time periods of the past, by using three different measurement systems mainly consisting of three different VNAs of the same type, three different frequency generators, and three different frequency counters. However, as the time was passed, a number of technical problems were arose from the desynchronization of automated measurements. So, to successfully resolve these problems, it was needed to appropriately reprogram our basic software application by which we coordinate the measurement devices participating in the VNA systems using the HP-IB interface. Well, under these circumstances we measured ten loads; the eight of a given uncertainty.

Keywords

Microwave measurements, network analyzer, differential error region, differential error interval, calibration, calibration standards

Introduction

It is well known that in order to take accurate measurements of the complex S parameters with a Vector Network Analyzer (VNA) it is absolutely necessary to perform calibration. Standard loads are used for this operation. Namely, for one-port measurements, the commonly used standards are the SLO standards, with nominal values for their reflection coefficient –1, 0, 1 respectively. From the one hand for the open load, we can leave the measurement port open with generally good - acceptable performance. From the other hand a short load is most easy to be constructed with great accuracy. Thus, what remains is the 50 Ohm standard load, which is the most difficult load since it is expected to have zero (0) reflection coefficient with undefined phase. Indeed manufacturers give significantly greater uncertainty for this load. It follows, therefore, that this load is of extreme importance for the measurements. A defective or damaged 50 Ohm standard load will produce undefined results for the unknown DUT.

With this fact in mind, we bought a number of used 50 Ohm HP 909A male loads and some other 50 Ohm loads, and together with our HP 909A male standard we performed a series of measurements with common the open and short loads. Thus, we formed different calibration sets which we applied to the measurement of the 50 Ohm-box [1] as the unknown DUT. All the measurements were performed with HP 8505A VNA in a period just before the NanoVNA era.

The presented comparison results were taken from measurements with three different HP 8505A VNAs, in different time and with different measurement systems. During this task several problems came out especially with the used external frequency generators. Solutions were given with appropriate changes in our software application for automated control of all the involved devices [2].

A short description of the three systems

a. The first system

The first measurement system was the type-N, $Z_0 = 50\ \Omega$, measurement system the one detailed described in [3]. This system is no more available since it was a university property. We repeat here, for completeness reasons, the specific used devices:

(i) HP8505A Opt 005PL VNA with
(ii) Opt 007 HP8501A Storage Normalizer,
(iii) HP8660C Synthesized Signal Generator with
(iv) HP86603 RF Section,
(v) HP5340A Opt 011 frequency counter,
(vi) a HP85032A 50 Ω Type-N Calibration Kit,
(vii)HP85032-60011Open/Short,
(viii) HP 8502 Transmission/ Reflection Test Set,
(ix) HP11501A-183 cm RF Cable, and

(x) HP-IB IEEE488 82335B/8-bit ISA Interface Card under the control of an AMD486/66 PC. This system operated from 1 to 1300 MHz with 100 Hz PLL stability in CW (non-sweep) frequency mode, full automated using a software application developed by us with Visual Basic 3.0 under Windows 3.11 [2].

All the initial measurements of the 50 Ohm-box was carried out with this system and which constituted a very good basis for the measurements with all the systems used by the antenna research group in the following years.

b. The second system

The second system was a type-N/APC-7, $Z_0 = 50\ \Omega$, measurement system with the following devices:

(i) HP8505A Opt 005PL VNA with
(ii) Opt 007 HP8501A Storage Normalizer,
(iii) HP8660C Synthesized Signal Generator with
(iv) HP86603A RF Section (1-2600 MHz),
(v) HP5340A Opt 011 frequency counter
(vi) HP11512A Short Load,
(vii) HP909A type-N male 50 Ohm standard load,
(viii) HP8503A S-parameter Test Set with APC-7 output connectors,
(ix) HP11524A APC-7 to type-N female adapter
(x) HP-IB IEEE488 82335B/8-bit ISA Interface Card under the control of an AMD486/66 PC. This system operated from 1 to 1300 MHz with 10 kHz PLL stability in CW (non-sweep) frequency mode.

All the devices were second-hand and an extensive period of tests was needed in order to make reliable measurements. Thus, we first changed all the fuses on the VNA parts, having a damaged fuse on the Normalizer since it was not a slow-blow fuse. Anyway, we did not use this part of the VNA. Then a malfunction in CW mode was observed. Only CW ± Δf with Δf = 0 was possible and that was a real problem for us. Fortunately the test for communication via the HP-IB interface was successful with both listen and talk functioning and with CW mode in order. The next tested device was the frequency counter which we finally abandon, since its performance was not stable over the whole frequency range, there was a big delay to respond via the HP-IB interface and although its role was auxiliary but enough important for the accuracy of the locked frequency on VNA, it was the one that made almost impossible to the whole system to operate normally.

The most critical device was the Synthesized Signal Generator since the stability and accurate determination of frequency on VNA was depended on it. Various tests were performed but although it seemed to communicate via HP-IB however the first attempt of automated measurements failed. It was obvious that the Phase Lock Loop could not be established. We made measurements manually (12 frequencies, from 2 to 1289 MHz with step 117 MHz) and we noticed that the VNA’s Source was stable enough. A comparison of those measurements with our third system and with the initial results for the 50 Ohm-box, as will demonstrate in the next section, was very promising that the system could operate well. After that we checked the signal level of the Generator and we found it rather low. With an oscilloscope we observed that the sinusoidal signal of the Generator was right, as well as the VNA’s Source. We put them all again to operate and we noticed that the frequency output of Generator was fluctuating. The decision was to increase the signal level both of the VNA’s Source and of Generator via HP-IB interface. And that was the solution. Obviously the frequency was now locked and the signal level was good, as shown in Tab. 1 for some tests via HP-IB interface. Thus, the only issue was to stabilize the output frequency of the Generator using a procedure analog to the one used for the VNA’s Source. A subroutine for the frequency feedback to the Generator was written. The frequency counter was now connected such as to show Genera-tors’ frequency and not that of the VNA and not in remote control. Several delays were added to the program in order to give more time to the VNA to talk after frequency lock. The flow graph of the feedback routine is shown in Fig. 1, where:

fr: the frequency sent to the Generator

fa: holds the integer value of fr

Nsource(fa): subroutine that sends the value fa to the VNA’s Source which talks for the first time

fb: keeps the value of fa

fi: the frequency from the Source - talk second time

ifd: the absolute value of the difference between the initial frequency with that of the Source

0.01: the frequency accuracy as it is exported from the VNA’s Source after talk. Two explicitly stated "if ... then" commands are used. When the frequency counter was part of the system this accuracy was 0.0001, which is a significant difference between our old first system with this one. Thus, at the end of the loop we add to the initial frequency half of the difference and send it again to the Generator via [gener] subroutine.

c. The third system

The third system was a type-N/75Ω, Z_0 = 50 Ω, measurement system with the following devices:

(i) HP8505A Opt 005PL VNA with
(ii) Opt 007 HP8501A Storage Normalizer,
(iii) HP8644A Synthesized Signal Generator, Opt 002, REV. 2, 0.25 - 2060 MHz
(vi) HP11512A Short Load,
(v) HP909A type-N male 50 Ohm standard load,
(vi) HP8503B S-parameter Test Set with 75 Ohm output connectors,
(vii) HP 11852A Minimum Loss Pad, 5.7dB, dc - 1.3 GHz, 50 Ohm N(f)/75 Ohm N(m) adapter,
viii) HP-IB IEEE488 82335B/8-bit ISA Interface Card under the control of an AMD 486 /66 PC. This system operated from 1 to 1300 MHz with 10kHz PLL stability in CW (non-sweep) frequency mode.

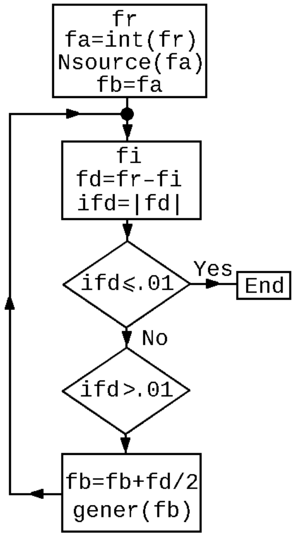

Fig. 1: Frequency feedback routine for Generator

Tab. 1: Frequency lock with signal level ~ −16dBm

VNA Source	Generator	open measurement
2.01	3.07	−00172E−2 −0055E−1
119.01	119.83	+00000E−2 +0146E−0
236.00	236.85	−00004E−2 −0714E−1
358.01	353.83	−00007E−2 +0701E−1
470.00	470.25	−0022E2−2 −0145E−0

Many tests were carried out, as was the case for the second system, as the devices were also second-hand. Measurements were taken manually from the VNA alone in 12 frequencies from 2 to 1289 MHz with step 117 MHz with a very good agreement with the initial results for the 50 Ohm-box. But when we tried to use the HP-IB interface the Processor unit could not "talk". Searching the manuals showed that three parts were involved:

A3A19: 08505-60017: Signal Processor I/O Storage Assembly

A3A20: 08505-60018: Signal Processor I/O Control Assembly

A3A21: 08505-60019: Signal Processor HP-IB Buffer Assembly

The A3A20 card was the most likely to have problem. We did find such a card to an old damaged unit from ebay and we exchanged it and the communication via HP-IB was restored. Both talk and listen were working fine again.

Since the external generator was totally different we had to change the related routines in our application in order to achieve its smooth communication with the VNA via HP-IB and we increase the delay between successive talks of the VNA’s Processor from 360 to 600 msec. Several test were made by varying the output signal level on the generator. We took measurements of the 50 Ohm-box with 0dBm and 10dBm. A small disturbance appeared at the measurements thus we repeated the whole procedure with our second minimum loss pad. The results will be presented in the next section.

Initial test measurements

The first results shown in Fig. 2 concerns the measurements that were taken manually for both the 2nd (#2-M) and the 3rd (#3-M) system in comparison with those of the 1st system (#1) for the 50 Ohm-box with full one port calibration. In addition the corresponding automated measurements by the 2nd system (#2-A) are shown, where the CW mode was possible via HP-IB as mentioned above. The vertical lines represent the DEIs of these measurements. For the 2nd and 3rd systems the signal level on VNA was −10dBm and on the Test Set 0dBm with the Vernier at −12 dBm and frequency range from 2 to 1289 MHz with step 117 MHz. The different Test Sets HP8503A and HP8503B respectively required the use of different adapter: APC7/N-f and Minimum Loss Pad 50 Ohm N(f)/75Ohm N(m) respectively. Other settings were: Range MHz: 0.5 - 1300, Mode: Lin-Expand, Width: CW ± Δf, Δf = 0 and CW for 2nd and 3rd system respectively, Trigger: Line, Scan Time sec: Min 0.01, Marker 1. The results were very good for both systems.

Fig. 3 shows our first failed attempt to take automated measurements from system 2, in the range 800 - 1200 MHz with step 20 MHz. There is clearly an unjustified variation which is attributed to the fact that essentially the measurements of the three standards and the DUT were not taken at the same frequency since the phase-locked loop was not functioning. Fig. 4(a) shows the difference between the measurement frequency of each of the four loads and the base frequency, ΔF [MHz], with RGB color for the SLO standards and in black for the DUT. Figs. 4(b) and 4(c) shows for the same frequency range what was expected to be these differences if the frequency lock was functioning correctly. The differences must take the values -0.01, 0. and 0.01, since this is the available lock accuracy (0.01 of MHz) for the 2nd system. Thus, it is obvious from Fig. 4(a), that the range [-1., 1.] of MHz does not guarantee reliable measurement results.

Fig. 5 shows a comparison of the 50 Ohm-box input impedance from the 1st system after calibration using as Open load: i) the open port of the test set with black color and ii) the open standard load mentioned above in red. Obviously, there is no significant difference between the results, thus we decided to leave the measurement port open during the calibration procedure for the O load.

Fig. 6 shows the results from the 3rd system using the same minimum loss pad to convert the 75 Ohm type-N test port to 50 Ohm type-N female, and 0dBm signal level at the Synthesized Signal Generator with red color while in green with 10dBm signal level. The differences between these two measurements and both with our reference in black color are almost negligible.

Finally, in Fig. 7 a comparison between the results for the 50 Ohm-box using 0dBm at the Generator and two different pads (1 in red and 2 in blue color) shows some slight differences which we should probably attribute to the second minimum loss pad. Furthermore, all the results from system 3 shows a small but visible discontinuity - "jump" at ~275 MHz, like those we have observed in NanoVNA H4 models [4], which after that experience may be attributed to the behavior of the second-hand HP8644A but further research is needed.

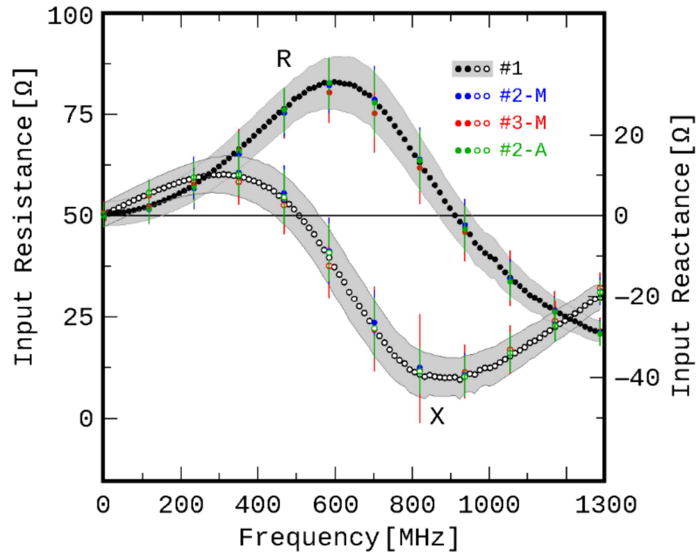

Fig. 2: First measurements with 2nd and 3rd system M for Manually taken measurements, A for Automated

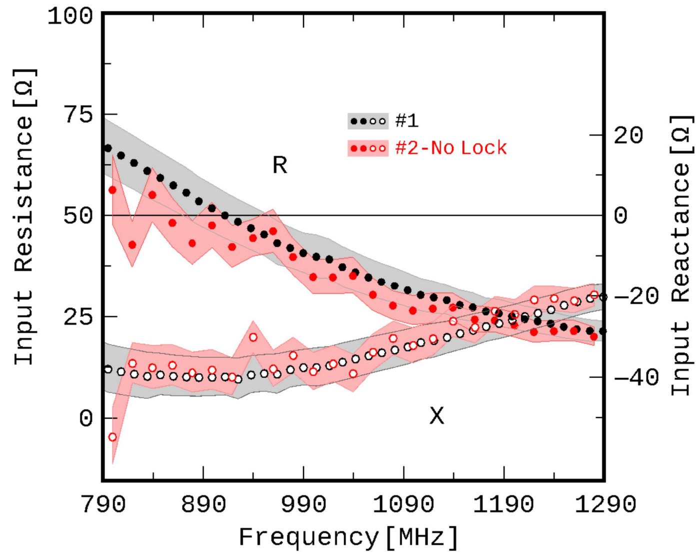

Fig. 3: System 2: Failed automated measurements

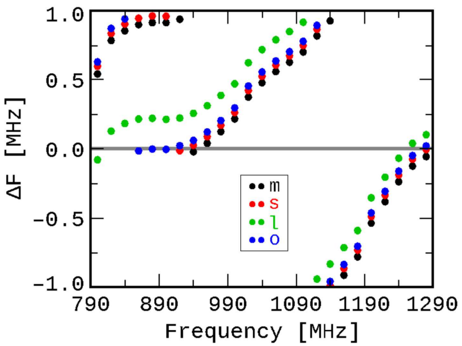

(a): No frequency lock

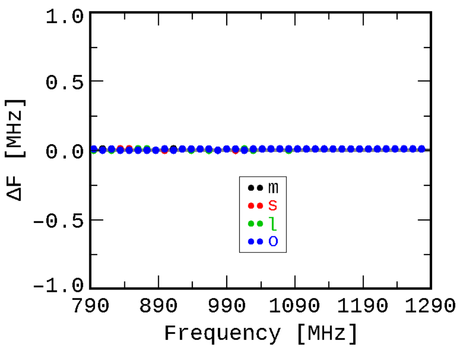

(b): Frequency lock

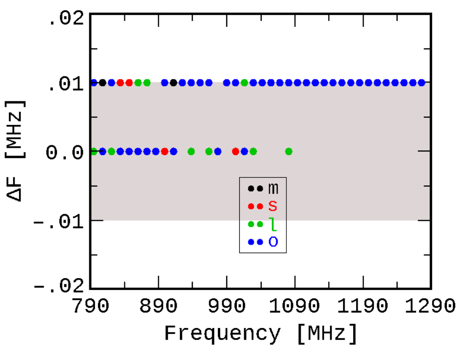

(c): Range [−0.01, 0.01]

Fig. 4: System 2: Frequency lock malfunction

Ten different 50 Ohm loads

The 2nd system was selected to measure ten (10) different 50 Ohm loads, all type-N male: (H1) the standard HP909A load that was used for a log period for our measurements and proved to be well behaved, thus it could be used as the reference load in order to characterize the others, (H2) a second-hand HP808A load, (H3) - (H8) six second-hand HP909A and (D1), (D2) two brand new NoName dummy loads. Initially we made the measurements of these 10 loads, the open and short for the calibration and of the 50 Ohm-box as DUT, supposing that all the 10 loads are good. Then we performed SLO calibration for each one of the 50 Ohm loads with common the open and short and extract the results for the DUT.

Fig. 8 shows the DUT reflection coefficient on the complex plane and Fig. 9 its input impedance, for all calibration sets. Obviously something went wrong. A measurement of the 50 Ohm loads with a simple multimeter proved that H2 had a dc value of 63 Ohm instead of a value near 50 Ohm and H8 showed 110 Ohm. Fig. 10 shows the comparison between DUT's input impedance from system 1 and after these two calibration sets from system 2.

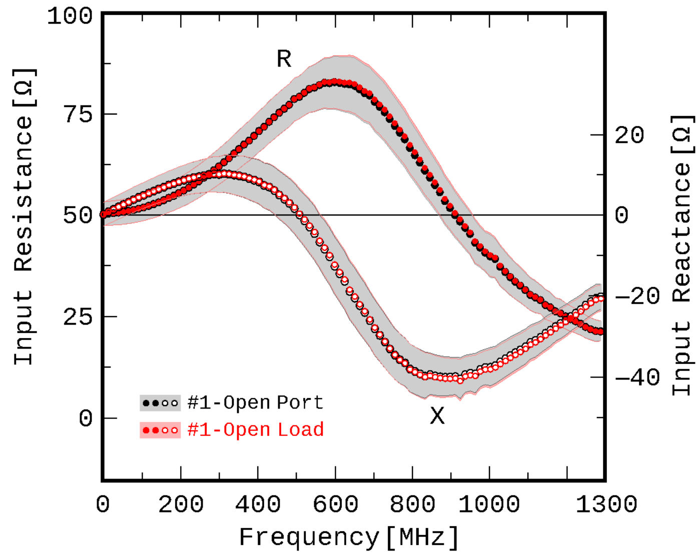

Fig. 5: System 1: Open port and Open standard load

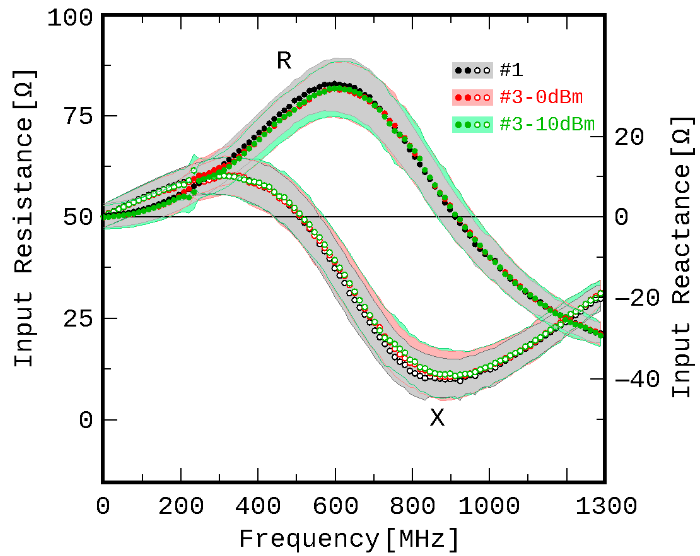

Fig. 6: System 3: 0dBm and 10dBm signal level on HP8644A

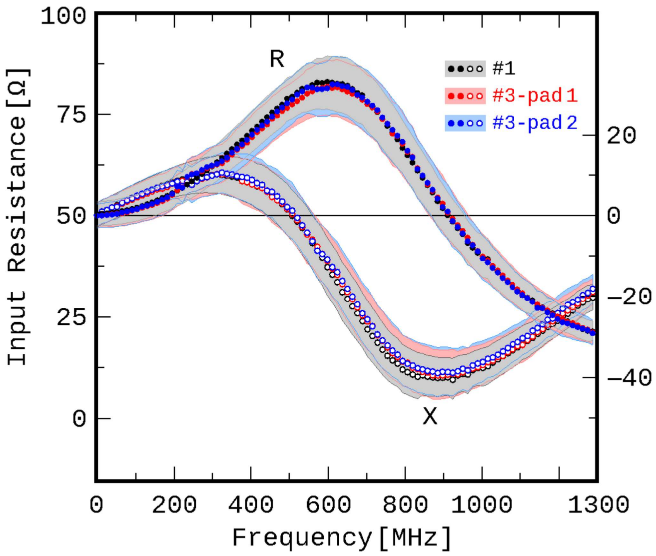

Fig. 7: System 3: Two different Minimum Loss Pads

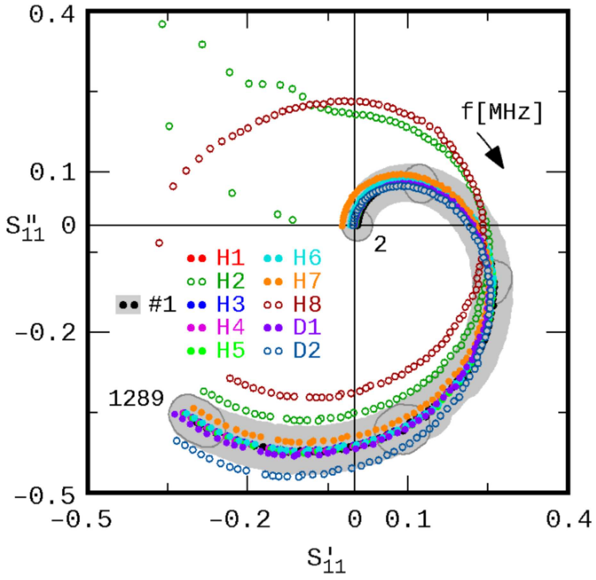

Fig. 8: DUT S_{11} after 10 sets of calibration

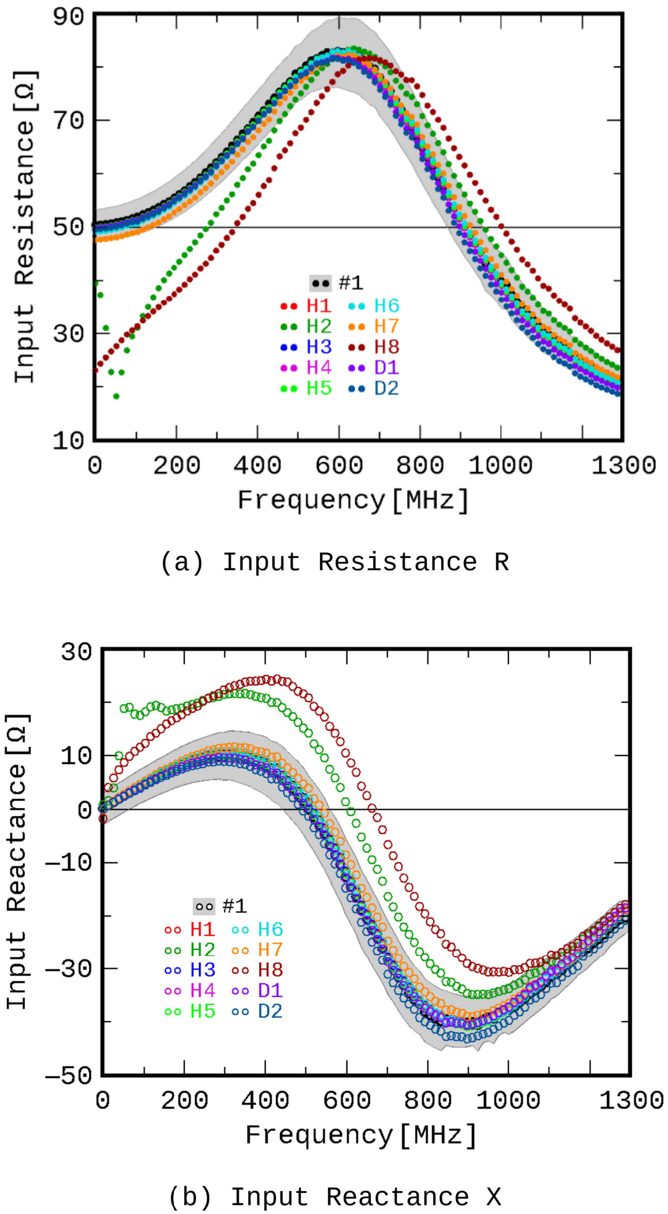

Fig. 9: DUT Z_{inp} after 10 sets of calibration

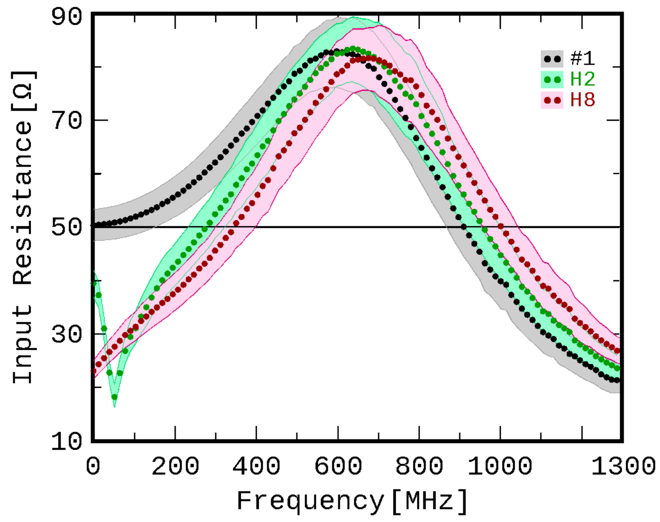

(a) Input Resistance R

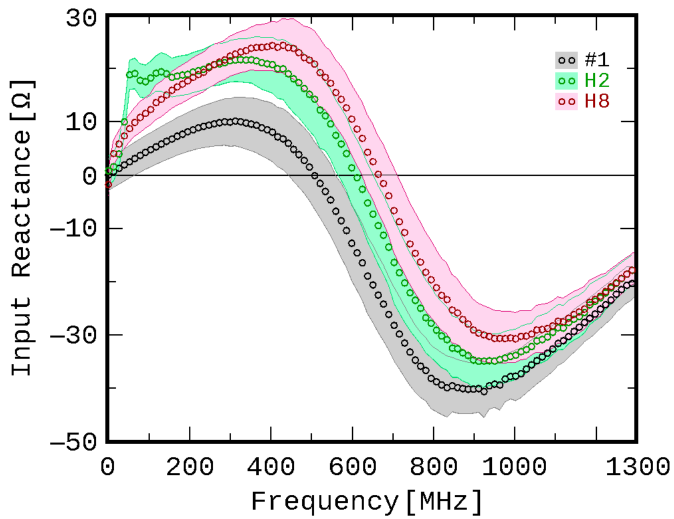

(b) Input Reactance X

Fig. 10: DUT Z_{inp} - from #1 and #2 when H2 and H8 faulty loads are used for calibration

In this figure, we have also added the corresponding DEIs for the three results of R, X to make it clear that under no circumstances could the measurements based on the loads H2 and H8 be accepted in order to characterize this specific DUT.

The next step was to use the so far well behaved standard load H1 as part of the calibration procedure and to face all the others nine (9) loads as DUTs. The results for their reflection coefficient are given in Fig. 11 on the complex plane. The corresponding input impedance is shown in Fig. 12. For a 50 Ohm load we expected a value near 0 for S_{11}, near 50 Ohm for the real part R and near 0 Ohm for the imaginary part X of its input impedance Z_{inp}. The accepted interval for S_{11} is represented with the gray circle of 0.029 radius, a value that corresponds to the 1.06 SWR available for the HP909A load [5] and a ±~3 Ohm for R represented as a gray strip in Fig. 12. The manufacturer of the two NoName dummy loads had provide no information about their uncertainty and the HP808A load has a little less SWR of 1.05 [6].

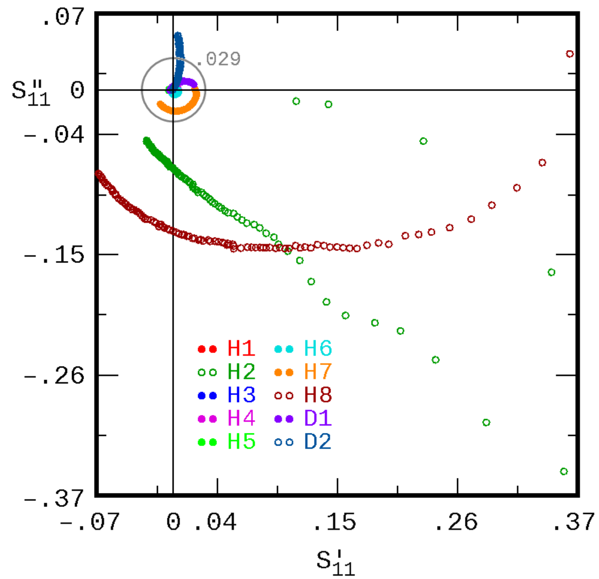

Fig. 11: S_{11} of loads as DUTs

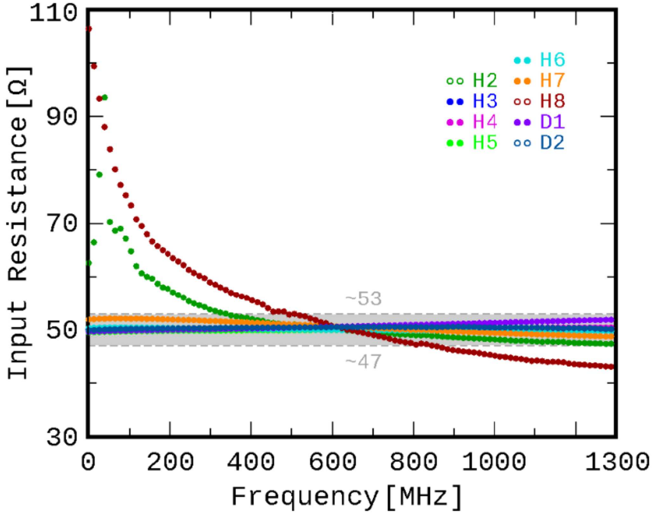

(a) Input Resistance R

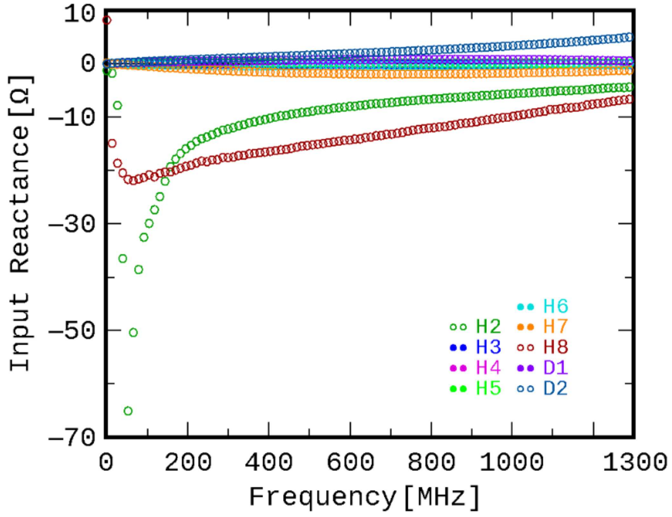

(b) Input Reactance X

Fig. 12: Z_{inp} of 9 loads as DUTs

In order to take a closer look to the behavior of the other seven (7) loads we redraw Fig. 11 excluding H2 and H8. Thus, from Fig. 13 as a first step the dummy load D2 can be excluded immediately, since it is out of the 0.029 circle for higher frequencies and as a second step by visual inspection the significant greater range of values for the other dummy load D1 and for the H7 load drives us to further remove these two loads. Fig. 14 shows the rest four (4) loads H3, H4, H5, and H6. They all have reflection coefficient values near the nominal value of 0 and could be characterized as good loads. However, trying to classify them, we created Fig. 15 for the magnitude of their input impedance as a function of frequency and Fig. 16 for the euclidean distance of their input impedance from 50 Ohm, d_{50}, based on the relation

$$d_{50} = \sqrt{(50 - R_i)^2 + (0 - X_i)^2} \qquad (1)$$

where i = 3, 4, 5, 6.

From Fig. 15, only with visual observation, we can again say that H4 and H6 appear as a little worse than the other two H3 and H5. But Fig. 16 is what orders them finally and essentially. The Mean Value (MV) of the distances throughout the examined frequency band shows that the loads H4 and H6 are of the same order and correspondingly H3 and H5 of the same, clearly better, order. With these data, we have chosen to keep apart these two loads and use the load H5, the better of all, as a replacement for our old H1 load. Fig. 17 shows the reflection coefficient of the 50 Ohm-box on the Smith Chart: (a) from system 1 and from system 2 using the three calibration sets with H1, H3 and H5 as 50 Ohm standards, (b) since the results are all too close, almost identical, only one stripe of DERs is shown and (c) the stripe of DERs and the result with H5 as 50 Ohm standard load.

Finally, it is worth to examine in more detail the readings of system 2 [7] on the complex plane in Fig. 18: (a) s, l (H1), o and m, (b) all Hi (i = 1, ..., 8) and D1, D2, (c) H1, (d) H3, (e) H4, (f) H5, (g) H6, (h) D1, (i) H7, (j) D2, (k) H2, (l) H8, with H1 to be present to all figures and the axes scales to be adjusted appropriately to make them better visible. It is evident even from these readings that the couples (H2, H8) and (H7, D2), are much different from the other loads, with a clearly greater value variation, far from what is expected for a good 50 Ohm matching load.

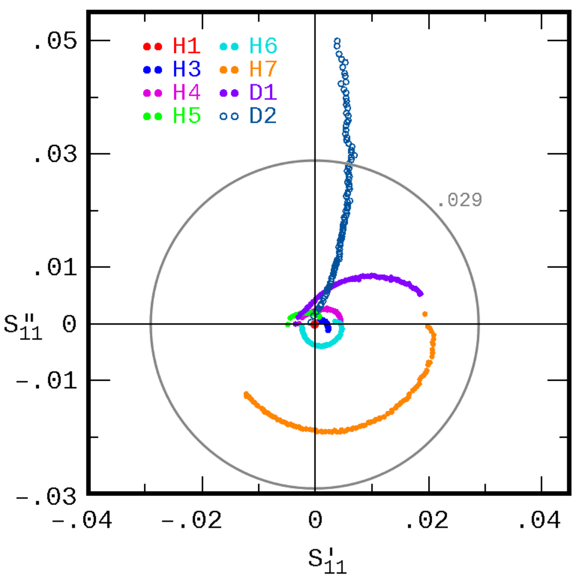

Fig. 13: S_{11} of 7 loads as DUTs with H1 as reference

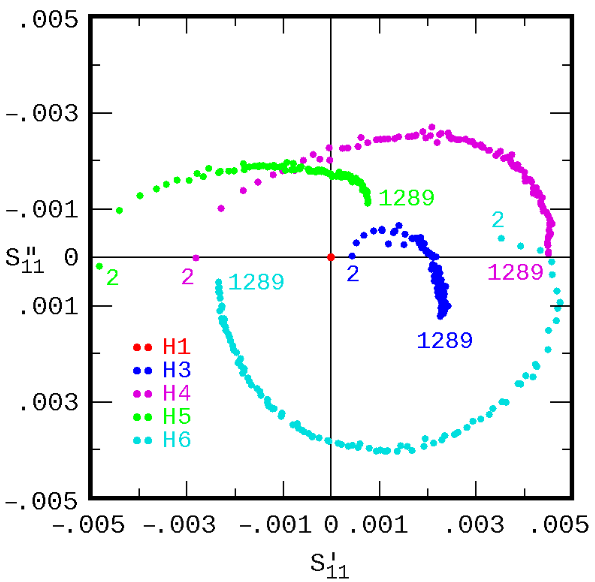

Fig. 14: S_{11} of H3, H4, H5, H6 as DUTs with H1 as reference

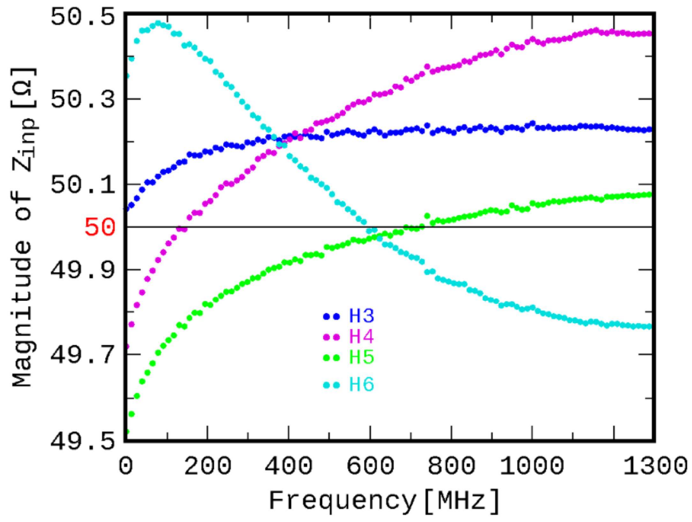

Fig. 15: $|Z_{inp}|$ of H3, H4, H5 and H6 as DUTs

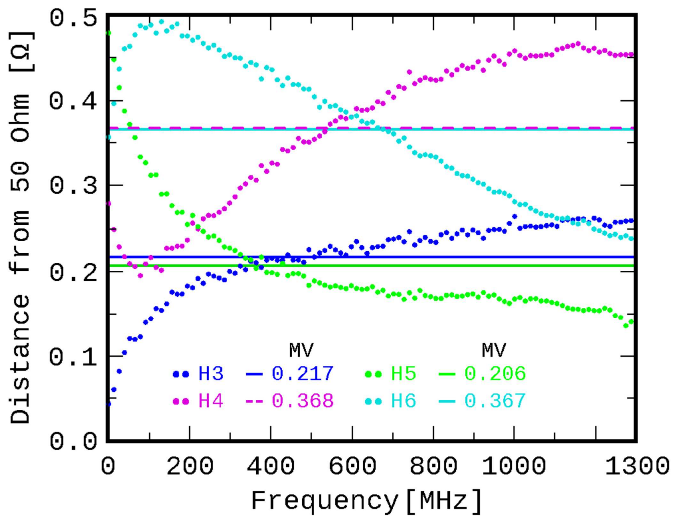

Fig. 16: d_{50} of H3, H4, H5, and H6 Z_{inp} with Mean Value (MV)

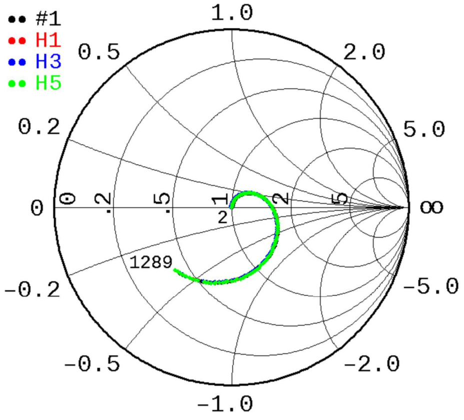

(a) ρ - 4 sets of calibration

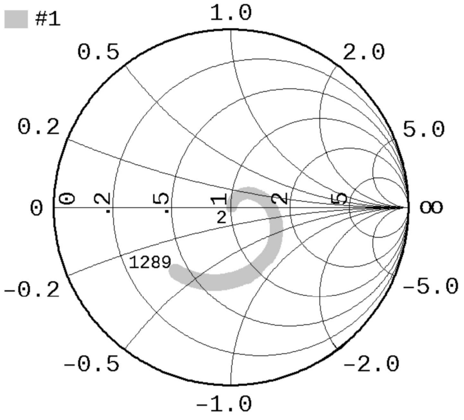

(b) ρ-DERs

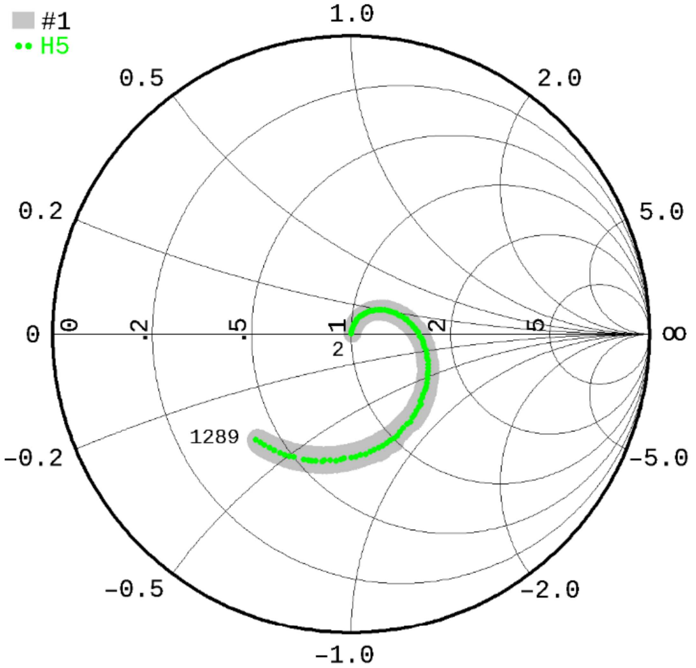

(c) ρ, ρ-DERs (H5 Load)

Fig. 17: Reflection coefficient ρ (S_{11}) on the Smith Chart

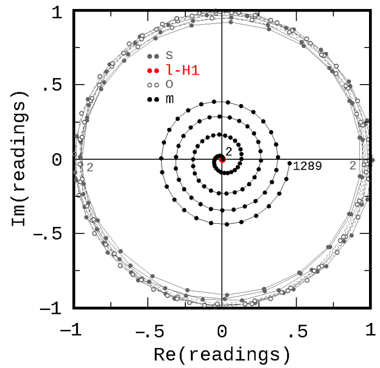

(a) s, l (H1), o, m

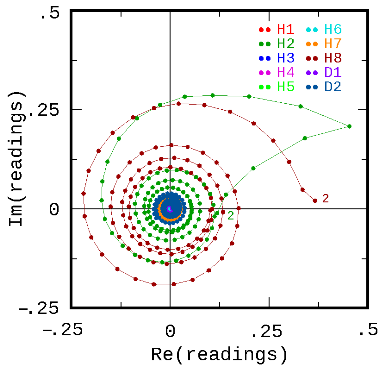

(b) Hi, i = 1, ..., 8, D1, D2

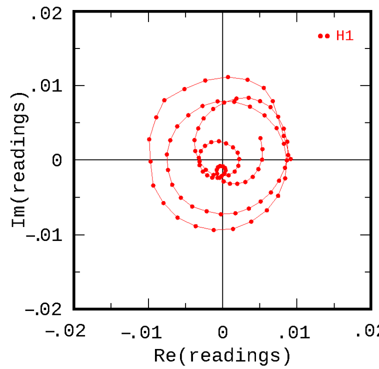

(c) H1

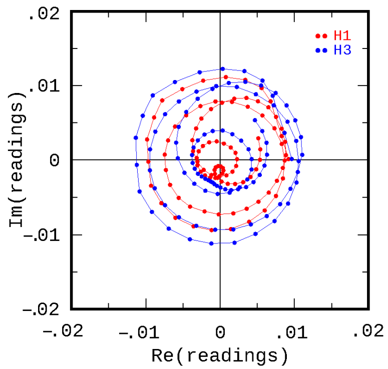

(d) H1, H3

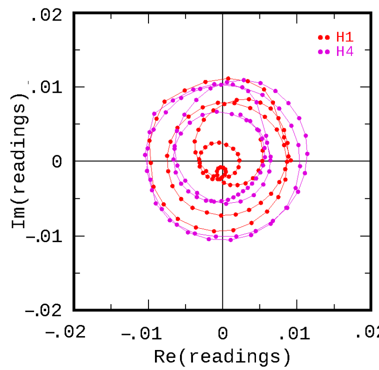

(e) H1, H4

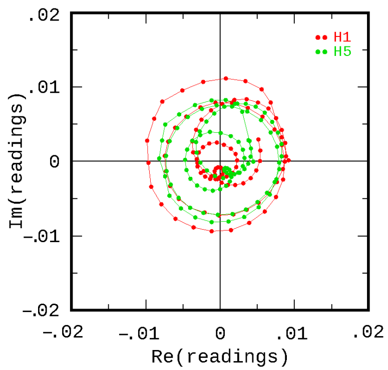

(f) H1, H5

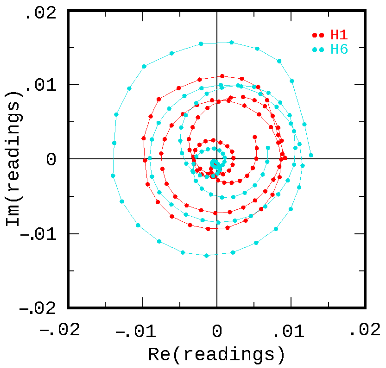

(g) H1, H6

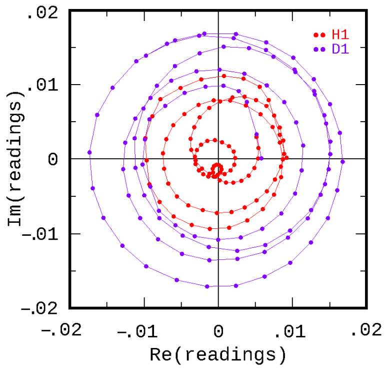

(h) H1, D1

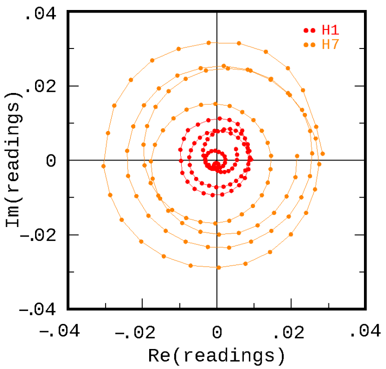

(i) H1, H7

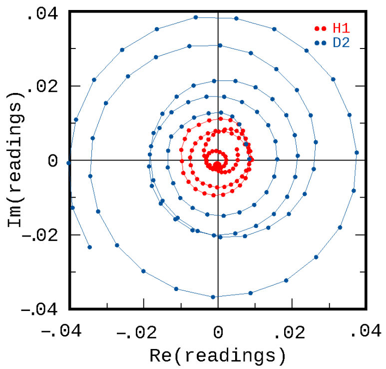

(j) H1, D2

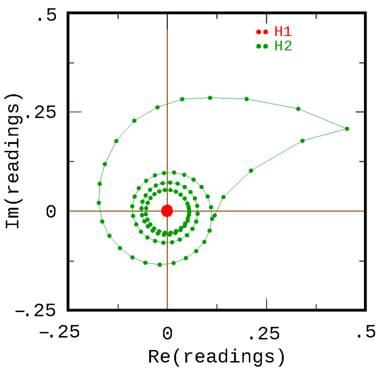

(k) H1, H2

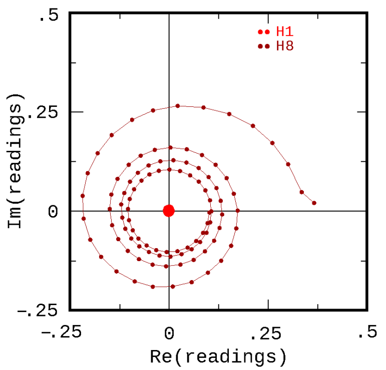

(k) H1, H8

Fig. 18: System 2: All the readings

H2, H8 problematic loads

In order to investigate if there is any way at all to use H2 and H8 loads as non-matching standard loads in a calibration procedure we need to use the full expression for their reflection coefficient, introduced in [8],

$$\rho = \frac{S(L-O)(ms+lo)+L(O-S)(ml+os)+O(S-L)(mo+sl)}{(L-O)(ms+lo)+(O-S)(ml+os)+(S-L)(mo+sl)} \quad (2)$$

where the small letters s, l, o, m corresponds to measurements and the capital letters S, L, O to standard loads. As already mentioned the short/open standards are the same, so S = –1 , O = 1 always and s, o are the same too. Furthermore, when the 50 ohm-box is the DUT m is the same for all calibration sets. The variables are the quantities L and its measurement l. Thus, we can rewrite the above expression as:

$$\rho = \rho(S, L, O, s, l, o, m) =$$
$$= \rho(-1, L, 1, s, l, o, m)$$

and by rearranging the fixed and variable terms

$$\rho = \rho(-1, 1, s, o; L, l, m) \quad (3)$$

and when the 50 Ohm-box is measured ρ becomes

$$\rho_{box} = \rho(-1,1,s,o,m_{box};L,l) \quad (4)$$

Fig. 19 shows the input impedance for the 50 Ohm-box as follows:

a) in black color from system 1 which was our reference with the corresponding Differential Error Intervals DEIs as light gray stripe where

$$\rho_{box} = \rho(-1,1,s,o,m_{box};0,l)$$

b) in dark green and dark red from system 2 with H2 and H8 respectively, as part of the calibration considered to have their nominal value of 50 Ohm, with their DEIs in light green and ligth magenta stripes respectively, where

$$\rho_{box}^{H2} = \rho(-1,1,s,o,m_{box};0,l_{H2})$$

$$\rho_{box}^{H8} = \rho(-1,1,s,o,m_{box};0,l_{H8})$$

c) in orange the result if we consider that they have a nominal value L as their first value at 2 MHz, when measured as DUTs which gives an impedance very close to the dc resistance measured with the multimeter, where

$$\rho_{box}^{H2} = \rho(-1,1,s,o,m_{box};\rho_{H2}^{1st},l_{H2})$$

$$\rho_{box}^{H8} = \rho(-1,1,s,o,m_{box};\rho_{H8}^{1st},l_{H8})$$

d) in magenta the result if

we consider that their nominal value L is equal to their average -Mean Value- across the entire zone when measured as DUTs, where

$$\rho^{H2}_{box} = \rho(-1,1,s,o,m_{box};\rho^{MV}_{H2},l_{H2})$$

$$\rho^{H8}_{box} = \rho(-1,1,s,o,m_{box};\rho^{MV}_{H8},l_{H8})$$

e) in light navy color the result if as L we use their measurement as DUTs, where

$$\rho^{H2}_{box} = \rho(-1,1,s,o,m_{box};l_{H2},l_{H2})$$

$$\rho^{H8}_{box} = \rho(-1,1,s,o,m_{box};l_{H8},l_{H8})$$

which is incorrect but is presented here for completeness, so as to include any possible misunderstanding case.

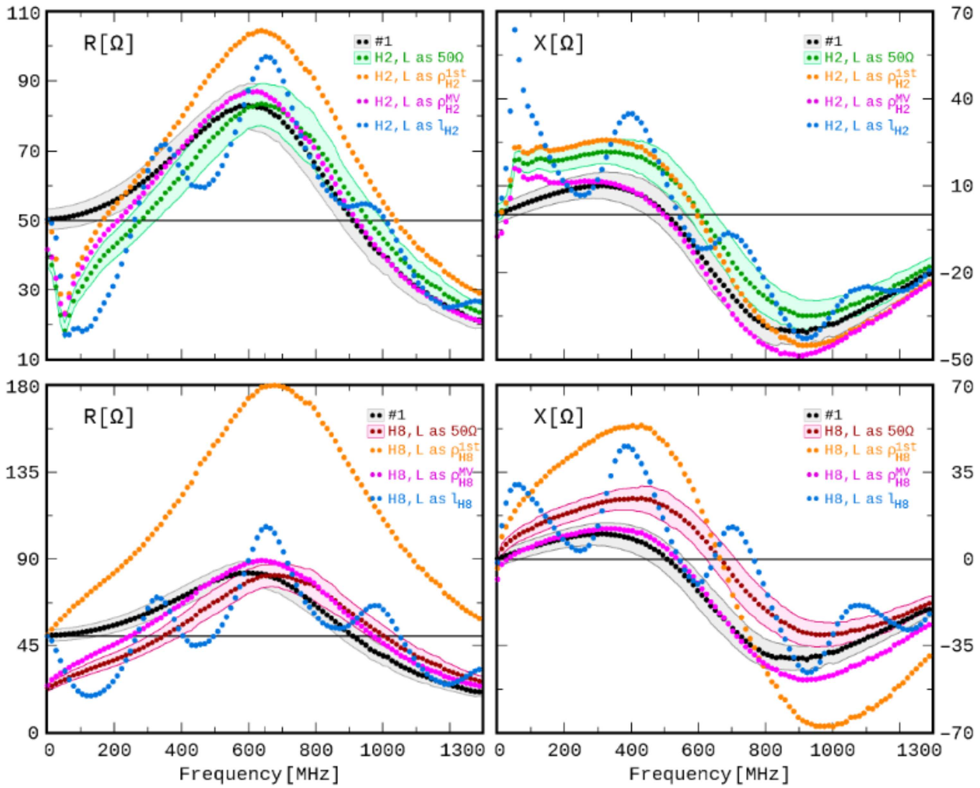

Fig. 19: Using faulty matching loads as calibration standards

Finally, Fig. 20 shows the input impedance for the 50 Ohm-box from system 2 with H2 and H8 respectively as part of the calibration considered to have their nominal value L equal to their ρ when they were measured as DUTs,

$$\rho^{H2}_{box} = \rho(-1,1,s,o,m_{box};\rho_{H2},l_{H2})$$

$$\rho^{H8}_{box} = \rho(-1,1,s,o,m_{box};\rho_{H8},l_{H8})$$

with

$$\rho_{H2} = \rho(-1,1,s,o,m_{H2},0,l_{H1}),$$

$$\rho_{H8} = \rho(-1,1,s,o,m_{H8},0,l_{H1})$$

Open points were used for the R, X of the box in order the result of the calibration set with the H1 good matching load to be visible.

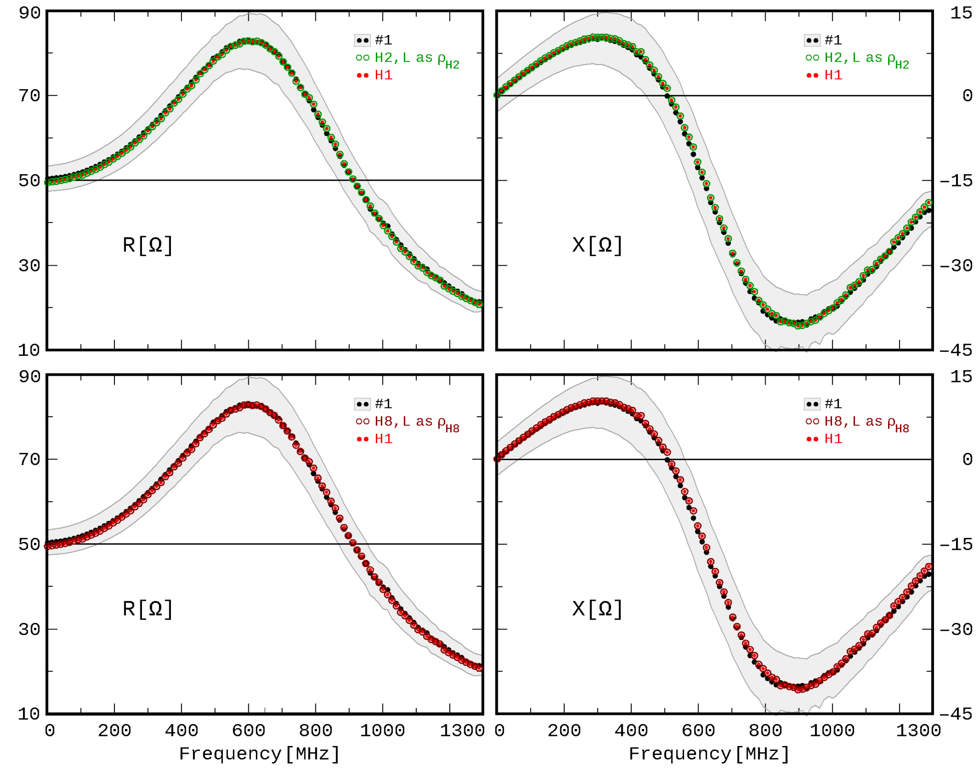

Fig. 20: Input impedance when L equals ρ_{H2}, ρ_{H8}

It is obvious that the results are exactly the same. This is due to the properties of the bilinear transformation. A substitution of ρ_{H2} in ρ_{box}^{H2}, ends up with the same expression as

$$\rho_{box} = \rho(-1, 1, s, o, m_{box}, 0, l_{H1})$$

which was verified by hand and mechanically by symbolically using Maxima and Mathematica CAS applications.

Conclusions

In 2014, we started a tedious, long term, process to built up from the scratch, the fourth research laboratory of ours (the previous at Thessaloniki, at Xanthi, and Antennas Laboratory), similar to a rather small subset of our Antennas Laboratory we founded at that pub univ dept, in order to stop at last parroting what others wrote about our subject, with a lot of what they said to be seemed at least insufficiently justified, if not totally irrational indeed, and using the just three years old then internet, to create, as early as 1996, pioneeringly open to the public online courses based on Virtual Reality [9], decisively serving thus The Cause of Teaching all the interested people and especially our students, not only theoretically, but also analytically and numerically, computationally and experimentally, the contemporary antenna results that we rationally confirmed by our own research work. However, a big, typically academic, pure envy arose against us, so that, already by the late 1993, after the stealing of our research notebook and hard disks from our research computer, by still unknowns even today, and under the tacit approval of the vast majority of our so called academic colleagues, as can be deduced from the absence of the slightest academic reaction from them, who, without ever asking officially about it, were definitely persuaded from an otherwise totally unjustified but unstoppable slander to our detriment, which although impressively unrelated to the actually produced research-teaching work by us, it was gave off from that systematically organized academic bunch of bullies and thugs, bosses of a crowd wanting a way out to pass course exams and grasp univ degrees, and regardless of our Nine Legal Recourses and Appeals to the Crime Courts and Supreme Administrative Courts and their corresponding decisions that were despised by the members of this gang, who stepped aside the whole of by duty competent authorities and managed to finally force me to Resign In Disgust as Permanent Assistant Professor of Antennas, sell out our house and household goods, and move out from Greece. In essence, as runaways from all those heavily toxic environments of them, we are now just intellectual self-exiles in the Real European Union [10]-[14].

Since these events occurred when the subject of this paper was not of high priority in our research interests, the above real facts explain not only the long delay in getting the research results we present today, but also the use of three different VNA systems to produce them. Additionally, we had to try very hard to finally find and ensemble the aforementioned VNA Systems 2 and 3, in such a way as to be as close as possible, at least namely, to the inaccessible, after 2014, VNA System 1, we used in our Antennas Laboratory of the past.

Moreover, various technical problems arose from the compulsory use of several, all second-hand, devices in our VNA Systems 2 and 3 that we could cheaply buy from private ebay sellers, since they needed serious maintain in the way presented above.

Generally speaking, these were the real conditions under of which we collected and used for the needs of this research work 10 loads in total, all of the same Type-N Male connector having nominal value 50Ω:

8 Matching Standards:
7 HP 909A, plus
1 HP 908A , and
2 NoName Dummy Loads,

the measurements of which drove us to the following summarized remarks:

A. Each standard load must be directly examined, before its use in a VNA measurement system, for its degree of compliance with its nominal specifications. Thus, for a 50 Ohm matching standard, we expect reflection coefficient values as close as possible to zero, for its magnitude or, in any case, within its uncertainty circle, as it is specified by its manufacturer - if it has any such characteristic known at all, since, as we already saw, no such specification exists for any of the two NoName Dummy Loads.

In addition, this behavior of the load should be as uniform and smooth as possible, that is, it must be substantially constant, in the whole of the frequency range of VNA measurements, in order to be appropriate for its calibration, so the usable frequency range of a load must also be a known characteristic of it.

However, as we already seen above, this demand, either as characteristic or as fulfillment, does not apply to all of the considered loads.

B. In the indirect estimation of appropriateness for calibration of all loads, we used each of them as the one of the needed three participating loads in the full one-port VNA calibration, while the other two were always the same, short and open, loads, for the following next measurement of our one-port 50 Ohm DC reference box constructed by us, that we considered as an unknown DUT in order to comparatively study the results for all loads.

C. After all that, the measured ten loads were ordered in terms of decreasing appropriateness for calibration, as follows:

0: Load H1, the one that was used as the base for all other measurements with system 2,

1-2: Loads H5 and H3, they proved as very good indeed,

3-4: Loads H6 and H4, having only a slightly decreasing behavior,

5-6: NoName Load D1, which was a pleasant surprise indeed, as it is just a Dummy Load, but along with Load H7, they have their ρ values always within the uncertainty circle of 0.029, as it was shown in Fig. 11 and Fig. 13, respectively,

7: NoName Load D2, the second Dummy Load, which although it is also a very good load in lower frequencies, unfortunately enough it goes out of the 0.029 uncertainty circle in the higher frequencies,

8-9: Loads H2 and H8, the checked as problematic ones from the very beginning, were finally proved, after several measurement checks, useless as calibration loads, at least under the currently considered conditions regarding their hypothetical values by us.

D. Thus, the question about the possibility of using a defective or damaged load as a matching or not matching calibration standard, answered negatively in this paper, since as it is shown in Fig. 19 all of our three attempts to somehow remedy their behavior directly, were unsuccessful.

E. At this point, we must emphasized once again that the results of unintended use of a more or less defective standard could lead to completely misleading conclusions regarding the behavior of a totally unknown DUT.

F. Finally, to experimentally demonstrate that it is impossible to get different results for our reference standard considering H2 and H8 as respectively having, each of them, its direct and intermediate values, which are different, we present this fact by showing the clearly identical measurement results in Fig. 20, although, as we mentioned above, we already knew this identity algebraically.

However, we keep our reservations regarding the identity of the corresponding to these different values DERs, which we define and estimate analytically. But this is interesting issue it has to be examined in another paper.

References – Updates – MD5 check

https://www.ftpj.otoiser.org/refs/382.htm

[1] Yannopoulou N.I., Zimourtopoulos P.E., "Measurement Uncertainty in Network Analyzers: Differential Error Analysis of Error Models Part 1: Full One-Port Calibration", FunkTechnikPlus # Journal, Issue 1, Year 1, 2013, pp. 17 - 22

https://ftpj.otoiser.org/refs/382.htm#r1

ftpj.otoiser.org/issues/html/ftpj-issue-01-e4-lo4104-pdfc171-ia1.htm#r12 (1-2)

[2] Yannopoulou N., Zimourtopoulos P., "ANALYZE: Automated Antenna Measurements, ver. 13", Antennas Research Group, 1993 - 2008

[3] Yannopoulou N., Zimourtopoulos P., "Total Differential Errors in One-Port Network Analyzer Measurements with Application to Antenna Impedance", Radioengineering, Vol. 16, No. 2, June 2007, pp. 1 - 8

https://ftpj.otoiser.org/refs/382.htm#r3

radioeng.cz/fulltexts/2008/08_01_01_08.pdf

[4] Yannopoulou N.I., Zimourtopoulos P.E., "Comparing a NanoVNA with a LabVNA Part2: Three NanoVNAs, Two H4 NanoVNAs, and One HP 8505A VNA", FunkTechnikPlus # Journal, Issue 36, Year 12, 2025, pp. 57 - 77

https://ftpj.otoiser.org/refs/382.htm#r4 ftpj.otoiser.org/issues/html/ftpj-issue-36-lo7532-export-ia1.htm#r363 (36-3)

[5] Keysight Technologies Inc., "909A Coaxial Termination DC to 18 GHz"

https://ftpj.otoiser.org/refs/382.htm#r5

keysight.com/dk/en/assets/7018-03039/technical-overviews/5990-8462.pdf

[6] Hewlet Packard, HP908A, 909A Coaxial Termination dc-18 GHz, Technical Data"

https://ftpj.otoiser.org/refs/382.htm#r6

testmart.com/webdata/mfr_pdfs/KEYSIG/5952-0919E.pdf

[7] Yannopoulou N.I., Zimourtopoulos P.E., "Measurement Uncertainty in Network Analyzers: Differential Error Analysis of Error Models Part 3: Short One-Port Calibration - Comparison", FunkTechnikPlus # Journal, Issue 2, Year 1, 2013, pp. 41 - 49

https://ftpj.otoiser.org/refs/382.htm#r7

ftpj.otoiser.org/issues/html/ftpj-issue-02-e4-lo4104-pdfc171-ia1.htm#r23 (2-3)

[8] Yannopoulou N.I., Zimourtopoulos P.E., "Comparing a NanoVNA with a LabVNA Part 1: One-Port Measurements", FunkTechnikPlus # Journal, Issue 34, Year 11, 2024, pp. 7 - 41

https://ftpj.otoiser.org/refs/382.htm#r8

ftpj.otoiser.org/issues/html/ftpj-issue-34-lo7532-export-ia1.htm#r341 (34-1)

Additional References

[9] Yannopoulou N.I., Zimourtopoulos P.E., "The Very First Ever Made 3D/4D Virtual Laboratory for Antennas", FunkTechnikPlus # Journal, Issue 3, Year 1, 2014, pp. 7 - 18

https://ftpj.otoiser.org/refs/382.htm#r9

ftpj.otoiser.org/issues/html/ftpj-issue-03-lo4104-pdfc171-ia1.htm#r31 (3-1)

[10] The stealing of our research work - 1993 (Hellenic)

https://ftpj.otoiser.org/refs/382.htm#r10

antennas.gr/Ka8arosF8onos/kloph.1993.gif

[11] The strangulation of our educational work - 2000 (Hellenic)

https://ftpj.otoiser.org/refs/382.htm#r11

antennas.gr/Ka8arosF8onos/straggalismos.2000.pdf

[12] The libel of an illegal student association against us - 2007 (English and Hellenic)

https://ftpj.otoiser.org/refs/382.htm#r12

antennas.gr/Ka8arosF8onos/illegal.2007.htm

[13] The legal establishment of our student association against that illegal student association - 2009 (Hellenic)

https://ftpj.otoiser.org/refs/382.htm#r13

antennas.gr/Ka8arosF8onos/legal.2009.html

[14] Since that's how they liked to live - 2008-2010 (Hellenic)

https://ftpj.otoiser.org/refs/382.htm#r14

antennas.gr/pub/yza/deece/

ARG NfP AoI
Antennas Research Group
Not-for-Profit Association of Individuals [*]
www.arg.op4.eu — arg@op4.eu
Scheiblingkirchen, Austria

* The Constitution of Greece, Article 12(3) — 2008:
  www.hellenicparliament.gr/en/Vouli-ton-Ellinon/To-Politevma
* The Hellenic Supreme Court of Civil and Penal Law:
  www.areiospagos.gr/en — Court Rulings:Civil|A1|511|2008

FRONT COVER VIGNETTE

A faded synthesis of an anthemion rooted in a meandros

The thirteen-leaf is a symbol for a life tree leaf.
"Herakles and Kerberos", ca. 530—500 BC,
by Paseas, the Kerberos Painter,
Museum of Fine Arts, Boston.

www.mfa.org/collections/object/plate-153852

The simple meandros is a symbol for eternal immortality.
"Warrior with a phiale", ca. 480—460 BC,
by Berliner Maler,
Museo Archeologico Regionale "Antonio Salinas" di Palermo.

commons.wikimedia.org/wiki/File:Warrior_MAR_Palermo_NI2134.jpg